Optimal Design of Multi-channel Water Cooled Radiator for Motor Controller of New Energy Vehicle

Zhu Zhang, Yunfan Liu, and Jingyuan Wang

***Abstract*—In order to improve the heat dissipation capability of motor controller for new energy vehicles, the water cooled radiator with multiple channels is optimized in this paper. The heat conduction between the heat source IGBT and the radiator, the convective heat transfer between the radiator and the coolant, the mechanical strength and the manufacturing cost are comprehensively considered during the optimization process. The power loss and thermal resistance of the IGBT unit are calculated at first, and finite element model of the radiator is established. On this basis, multi-physics coupling analysis of the water cooled radiator is carried out. Secondly, the sensitivity analysis is applied to verify the influence of structural parameters on the heat dissipation performance of the radiator system. The influence of coolant inlet velocity v, number of cooling ribs n, height of radiator ribs H on the maximum temperature rise T, the temperature difference ΔT between phase U and W, and the coolant pressure loss ΔP are analyzed in depth, and the optimal range of the structural parameters for heat dissipation is obtained. Finally, an experimental platform was set up to verify the performance of the proposed structure of water cooled radiator for motor controller of new energy vehicle. The results show that the heat dissipation capability of the proposed radiator is improved compared with the initial design.**

***Index Terms*—Motor controller; Water cooled radiator; Finite element method; New energy vehicle**

I. Introduction

THE power battery, drive motor and vehicle electronic controller are three core components of new energy vehicles. As an important part of vehicle electronic controller, the motor controller has the characteristics of high switching frequency, high power loss, high integration and high power density[1]. The reliability, safety and service life of the motor controller is guaranteed by the radiator with efficient heat dissipation capability[2]. Therefore, the optimal design of the heat dissipation system of the motor controller is of great significance for the efficient and safe operation of new energy vehicles.

In order to improve the power density, the driving motor and controller of new energy vehicles generally adopt liquid cooled method. The cooling system mainly relies on electric pumps to drive the coolant circulating in the cooling pipeline. Through the heat exchange of the coolant in the radiator, the heat generated by the motor and the controller is taken away. The cooling system is composed of electric pump, expansion tank, radiator and cooling pipe, as shown in Fig. 1.

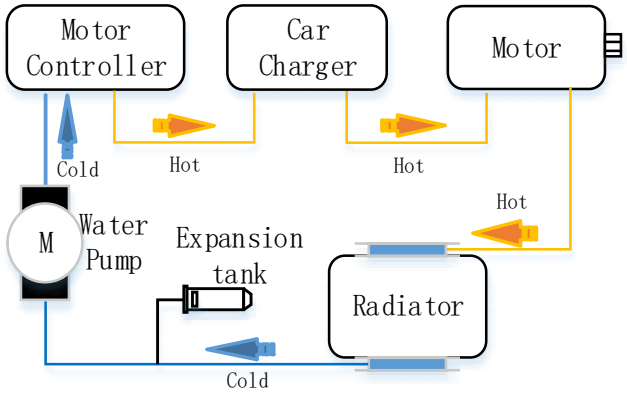

Fig. 1. Schematic diagram of water cooled system.

In order to meet the requirements of motor controller, the design optimization of heat dissipation system has been studied for the past decade. In [3], the design method of radiator ribs is studied by analyzing the power consumption of IGBTs, and it is concluded that corrugated radiator ribs are more conducive for heat dissipation than flat radiator ribs. In [4], the thermal parameters of the radiator under different working conditions and different cooling structures are calculated by the fluid analysis software, and the structural thermal stress and thermal strain of the thermal load were analyzed. The influence of the fin structure on the heat dissipation performance, thermal stress and thermal strain of the radiator is comprehensively analyzed, which provided a theoretical reference for the heat dissipation design of the motor controller for vehicles. In [5], three structural models of the cooling ribs in the flow channel of the water cooled radiator are designed, and the finite element software is used to simulate and analyze the temperature distribution of IGBT and

Manuscript received January 29, 2022; revised March 09, 2022; accepted March 14, 2022. date of publication March 25, 2022; date of current version March 18, 2022.

This work was supported in part by the National Natural Science Foundation of China (61503132).*(Corresponding Author: Yunfan Liu)*

Zhu Zhang is with the School of Information and Electrical Engineering, Hunan University of Science and Technology, Xiangtan, 411201, China (e-mail: eezhuzhang@126.com).

Yunfan Liu and Jingyuan Wang are with the major in power electronics, Hunan University of Science and Technology, Xiangtan, 411201, China(e-mail: 1185370836@qq.com; 13227232360@163.com).

Digital Object Identifier 10.30941/CESTEMS.2022.00012

the pressure loss of coolant under different flow parameters. The results show that the cooling ribs with streamline distribution have better heat transfer effect and lower fluid resistance, which is more conducive to the heat dissipation of radiator. In [6], the influence of the number of radiator ribs and the thickness of substrate on the heat dissipation effect of PEBB unit is determined by curve fitting, and the optimization scheme of the structure is given by calculating the extremum of the function. In [7], the influence of the size of a flat water cooled radiator on the heat dissipation effect is theoretically analyzed by using the unified dimension method, and the design optimization is carried out. It is concluded that the flat water cooled radiator with small channel size is more effective to solve the heat dissipation problem of large heat flux devices. Reference [8] studies the flow and heat transfer characteristics of fluid in rectangular/serrated and single/double-layer microchannels radiator, and it is concluded that the double-layer cooling channel is better than the single-layer structure, and the rectangular channel is better than the serrated channel. Although extensive researches have been carried out on the design of heat dissipation system, there are few studies on the water cooled radiator of motor controller for new energy vehicles. The heat dissipation efficiency, the temperature rise and temperature difference of IGBT modules need to be improved and optimized with the improvement of new energy vehicle requirements.

In this paper, the water cooled radiator system of a new energy vehicle motor controller is studied, and the structure of the radiator is optimized with multi-objectives. Firstly, the power loss of the IGBT modules is approximately calculated. Then, the water cooled radiator with different structural parameters is modeled with 3D modeling software. The models are imported into ICEPAK for multi-physical field finite element analysis of heat dissipation capability. The sensitivity analysis is carried out to obtain the optimal structure of the radiator. Finally, the experimental platform is built to verify the proposed optimization method for water cooled radiator of vehicle motor controller.

II. Power Loss Calculation of IGBT Module

The power loss of IGBT module is composed mainly of the on-state loss, switching loss of internal IGBT transistor and anti-parallel freewheeling diode FWD[9]. The loss of a single IGBT module is calculated as follow

$$P_A=P_Q+P_D=P_{SS}+P_{SW}+P_{DC}+P_{rr} \tag{1}$$

where P_A represents the loss of a single IGBT module; P_Q is the total loss of a single IGBT; P_D is the loss of a single FWD; P_{SS} refers to the conduction loss of a single IGBT; P_{SW} is the switching loss of a single IGBT; P_{DC} is the conduction of a single FWD Loss; Prr is the switching loss of a single FWD.

Therefore, the total loss of the power module in the controller can be calculated from

$$P_{\text{total}}=6P_A \tag{2}$$

where P_{total} denotes the total loss of the power module.

A. Power Loss of IGBT

The on-state loss of IGBT is caused by conduction voltage drop, which is related to current, voltage drop and modulation ratio[10]. The conduction loss of a single IGBT can be approximately expressed as

$$P_{SS}=\left(\frac{1}{8}+\frac{M\cos\theta}{3\pi}\right)\times V_{CEO}\times I_{CP} \tag{3}$$

where M is the modulation ratio; $\cos\theta$ is the power factor angle; V_{CEO} is the saturated voltage drop when the transistor junction temperature is 125 ℃ and the peak current is I_{CP}; I_{CP} is the maximum collector current at actual operation.

The switching losses of IGBT include switching losses and turn-off losses, which are related to switching frequency, current, bus voltage and gate resistance. The higher the switching frequency, the higher the proportion of switching loss in the total loss. The switching loss of a single IGBT can be expressed as

$$P_{SW}=\frac{1}{\pi}\times f_{sw}\times\left(E_{SW(on)}+E_{SW(off)}\right) \tag{4}$$

where f_{SW} is the switching frequency, $E_{SW(on)}$ is the energy lost once when the IGBT is turned on; $E_{SW(off)}$ is the energy lost once when the IGBT is turned off.

B. Power Loss of Diode

The conduction loss of the diode is related to the current, the conduction voltage drop, and the modulation ratio. The conduction loss of a single diode can be expressed as

$$P_{DC}=\left(\frac{1}{8}-\frac{M\cos\theta}{3\pi}\right)\times V_F\times I_{CP} \tag{5}$$

where V_F is the on-state voltage drop of the diode.

The diode switching loss mainly refers to the reverse recovery loss during the turn-off process, which is also related to the switching frequency, current, bus voltage and gate resistance. The diode switching loss can be expressed as

$$P_{rr}=\frac{1}{\pi}\times f_{sw}\times E_{D(off)} \tag{6}$$

where $E_{D(off)}$ is the reverse recovery loss of the diode.

III. Structure of Water Cooled Radiator

A. Structure of Motor Controller

In this paper, the motor controller of new energy vehicle is mainly composed of capacitor, IGBT module, connecting terminal, mechanical housing, and water cooled radiator. The

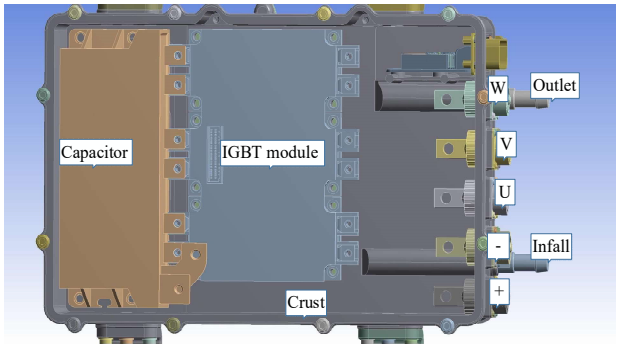

Fig. 2. Structure diagram of motor controller.

structure diagram of the motor controller is shown in Fig. 2.

Since the volume of water cooled radiator accounts for nearly 1/3 of the whole controller, reasonable selection of materials can not only effectively reduce the weight of the whole controller, but also effectively improve the heat dissipation rate and the working efficiency of the controller. Aluminum alloy material [11] is widely used in the production of heat dissipation equipment because of its high thermal conductivity, low density, high strength and good corrosion resistance. IGBT is an electronic equipment with high heat flux. In order to ensure its safety, reliability and service life, it is necessary to have an efficient heat dissipation system under its working state. Some studies have shown that the heat flux of microelectronic chips is generally 60-90 W/cm^2, and the maximum is more than 200 W/cm^2 [12].

B. Structure of Water Cooled Radiator

The internal structure of the water cooled radiator studied in this paper is shown in Fig. 3. The cooling liquid enters from the inlet, flows through the S channel and flows out of the outlet. Fig. 3(b) shows the cross-section diagram of the radiator. It can be seen that a number of parallel cooling ribs are uniformly distributed in each channel. Fig. 3(c) shows the distribution of cooling ribs in one of the channels. Such design increases the convective heat transfer area and the turbulence intensity of the coolant, which can make the heat dissipation efficiency higher[13].

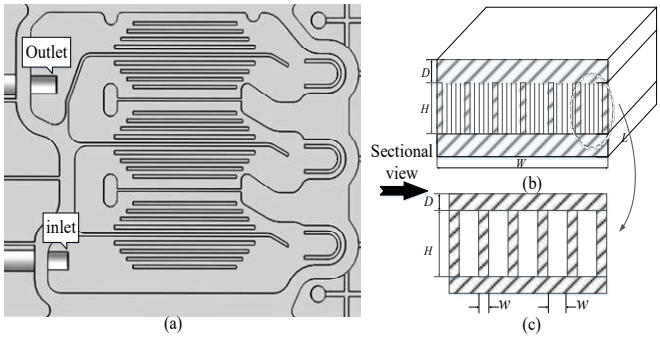

Fig. 3. Schematic diagram of water cooled radiator.

IV. Heat Dissipation Analysis of Motor Controller

A. Model Simplification

In this section, CAD software is used to model the cooling radiator. In order to improve the calculation speed and reduce the calculation time of the finite element analysis, the original model is reasonably and effectively simplified without affecting the authenticity of the overall model. The surrounding parts of the controller housing are removed, and some details such as chamfer, screw, screw hole and seal ring are ignored. The simplified 3D model is shown in Fig. 4.

B. Power Consumption Calculation

The IGBT used in the motor controller is FF450R12ME4 module produced by Infineon, and three modules constitute a three-phase inverter circuit. According to the rated parameters and control algorithm of the motor controller, the rated output current of the module is 145 A, the modulation ratio M is 0.9, and the switching frequency is 10 kHz. Therefore, the power

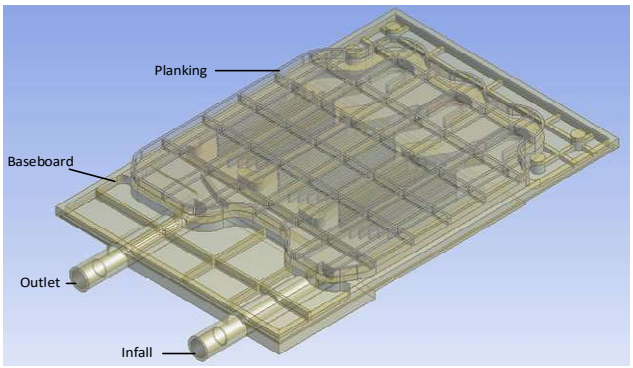

Fig. 4. Simplified model of water cooled radiator.

TABLE I
POWER LOSS OF IGBT MODULE

Parameter	P_{SS}/W	P_{SW}/W	P_{DC}/W	P_{rr}/W	P_A/W	P_{total}/W
Numerical value	58.5	119.0	10.5	123.2	311.2	1867.2

consumption of the IGBT module can be calculated as shown in Table I.

C. Heat Dissipation Simulation Calculation

The primary mode for heat dissipation of the radiator is forced water cooled, and the radiation heat dissipation between the radiator and the surrounding environment is ignored. The Reynolds number of the liquid in the flow channel is calculated to be much larger than 3000. Therefore, the fluid is set as a turbulent field, and the calculation domain is the fluid flow area in the radiator flow channel. The inlet temperature is set to 55, and the ambient temperature is defaulted to 20. The standard turbulence model is adopted in this paper.

The physical equation of the model is shown in (7) and (8).

$$\rho\frac{dk}{dt}=\frac{\partial}{\partial x_i}\left[\left(\mu+\frac{\mu_t}{\sigma_k}\right)\frac{\partial k}{\partial x_i}\right]+G_k+G_b-\rho\varepsilon-Y_M \tag{7}$$

$$\rho\frac{d\varepsilon}{dt}=\frac{\partial}{\partial x_i}\left[\left(\mu+\frac{\mu_t}{\sigma_\varepsilon}\right)\frac{\partial \varepsilon}{\partial x_i}\right]-C_{2\varepsilon}\rho\frac{\varepsilon^2}{K}+C_{1\varepsilon}\frac{\varepsilon}{k}\left(G_k+C_{3\varepsilon}G_b\right) \tag{8}$$

where : $C_{1\varepsilon}$=1.4; $C_{2\varepsilon}$=1.92; $C_{3\varepsilon}$=0.09; σ_k=1.0; σ_ε=1.3

G_b represents the turbulent kinetic energy caused by the influence of buoyancy; Y_M represents the effect of compressible turbulent pulsating expansion on the total dissipation rate; the turbulent viscosity ratio is given by (9).

$$\mu_t=\rho C_\mu k^2/\varepsilon \tag{9}$$

where C_μ is the empirical coefficient, usually C_μ = 0.09; k is the turbulent kinetic energy; ε is the turbulent energy dissipation rate.

The simulation parameters are set as follows. The cooling radiator and IGBT are solid and the material is selected as Al-Extruded. The IGBT modules are selected as the heat source, and the power is 1867 W. The fluid material in the radiator is set to water. The fluid-solid coupling algorithm is

used to solve the energy equation. The convergence accuracy is 10^{-7} and the iteration steps are 1000 steps. The advantage of this method is that the solution process is easier to converge and the error is smaller.

D. Sensitivity Analysis

The performance of motor controller is restricted by the maximum temperature rise of IGBT modules and the temperature difference among them. The performance is better when the maximum temperature rise of IGBT is lower under the same working conditions. Besides that, the heat dissipation capability is improved with smaller temperature difference between phase U-W. The inlet pressure is given by the electric pump. The pressure difference between the inlet and outlet is the pressure loss of the coolant in the radiator. The smaller the pressure loss is, the smaller the electric pump power required [14]. Therefore, the performance of the cooling radiator can be evaluated by the IGBT maximum temperature rise T_{max}, the temperature difference between U-W phase ΔT and the pressure loss between inlet and outlet ΔP.

1) The Influence of the Number of Water Channels on the Heat Dissipation Performance

Fig. 5 shows the curves of maximum temperature rise T_{max}, temperature difference between U-W phase ΔT and pressure loss between inlet and outlet ΔP with the number of radiator ribs. Due to the limitation of radiator width, only 8 radiator ribs can be added at most. With the increase of the number of heat sinks, the maximum temperature rise of IGBT begins to decrease, but when it increases to a certain extent, the maximum temperature will rise again. Because the number of

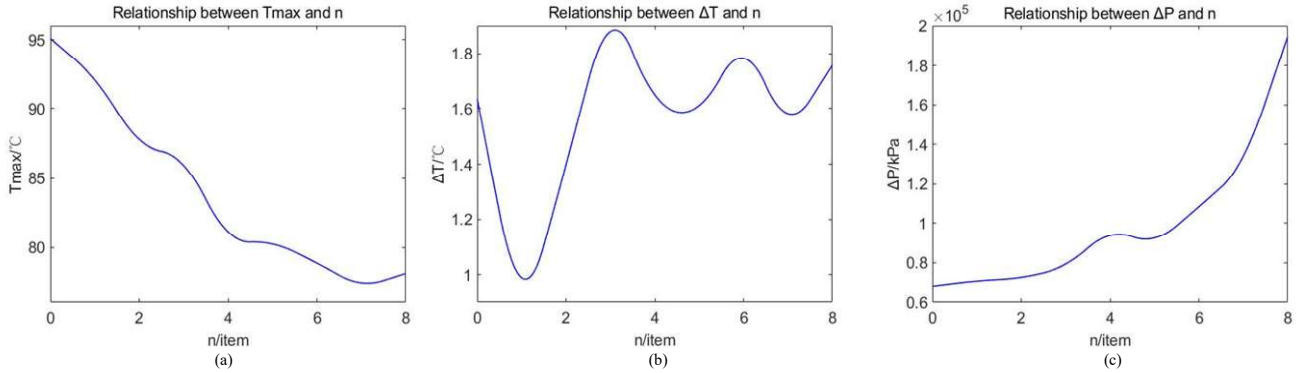

Fig. 5. The change of T_{max}、ΔT、ΔP with respect to n.

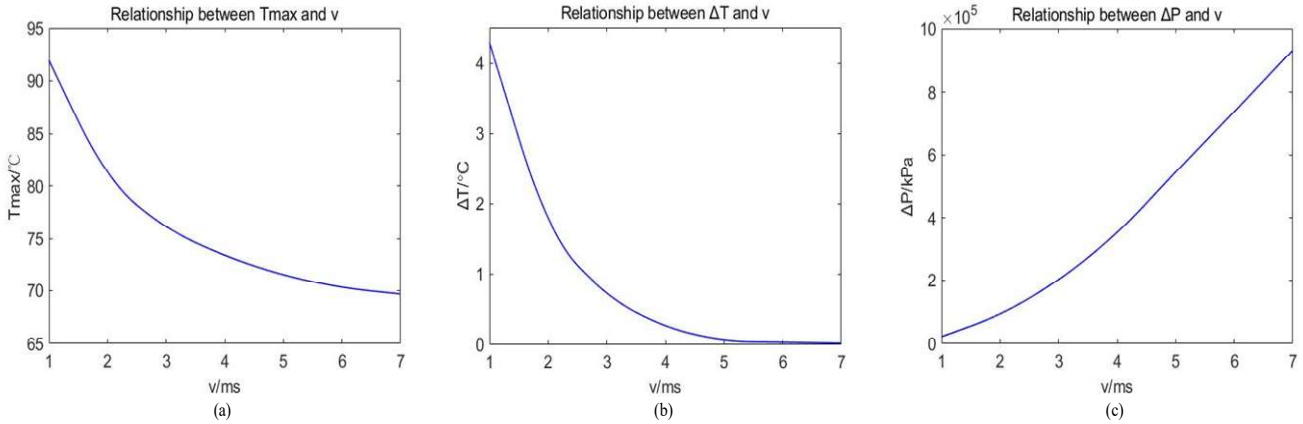

Fig. 6. The change of T_{max}、ΔT、ΔP with respect to v.

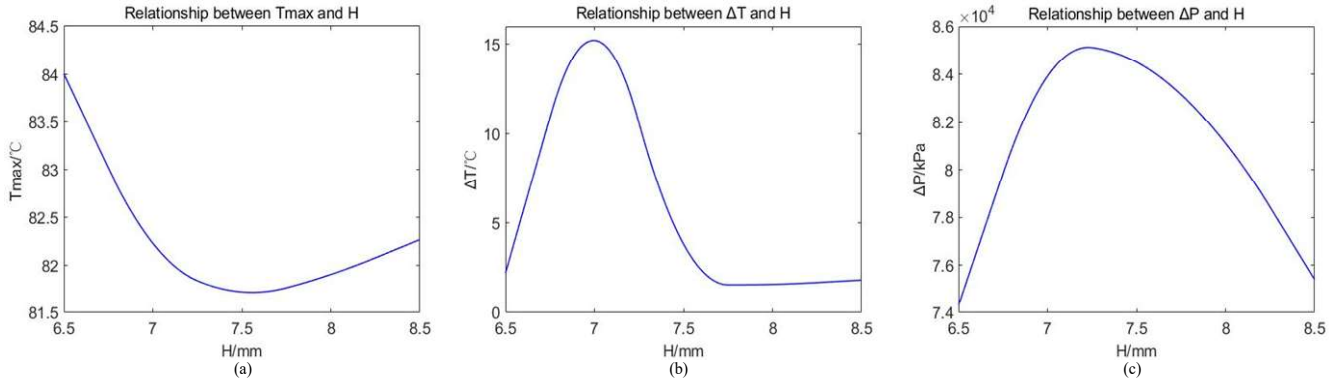

Fig. 7. The change of T_{max}、ΔT、ΔP with respect to H.

radiator rib is so many that hinders the flow of coolant, reduces the flow rate and the heat dissipation performance. The pressure loss is generally increased, but there is a relatively flat platform period when the number of cooling ribs is 4, and then it continues to rise. The temperature difference between U-W phase decreases at first and then increases with the increase of the number of radiator bars, and finally fluctuates around 1.7 °C.

2) The Influence of Inlet Flow Rate on Heat Dissipation Performance

Fig. 6 shows the variation curves of the maximum temperature rise T_{max}, the temperature difference between U-W phase ΔT and pressure loss between inlet and outlet ΔP with the flow rate of coolant. The higher the flow rate is, the lower the overall temperature of IGBT is, and the smaller the U-W phase temperature difference is. However, the pressure loss and the power dissipation of the electric pump is getting larger, resulting in higher power consumption of the whole cooling system.

3) The Effect of Heat Dissipation Rib Height on Heat Dissipation Performance

Fig. 7 shows the variation curves of the maximum temperature rise T_{max}, the temperature difference between U-W phase ΔT and pressure loss between inlet and outlet ΔP with the height of the radiator ribs. The height of the radiator ribs affects the flow mode of the coolant. With the increase of the height of the radiator ribs, the Nusselt number of the coolant is larger, the turbulence degree is higher, and the heat brought out by the coolant is more. Therefore, with the increase of the height of the radiator, the temperature of the radiator plate decreases. However, with the increase of the height of the ribs, the pressure loss is increasing at first and reaching the maximum value at the height of 7.2 mm, then it keeps decreasing.

V. Optimization Results and Experimental Verification

A. Optimization Results and Analysis

1) Optimization Function

According to the sensitivity analysis, the linear weighting method is used to transform the multi-objective problem into a single objective, and the optimal solution is determined by adjusting the weight of the objective function. The objective function can be expressed as

$$F_{obj}(v,n,H)=\omega_1\frac{T}{T_{\max}}+\omega_2\frac{\Delta T}{\Delta T_{\max}}+\omega_3\frac{\Delta P}{\Delta P_{\max}} \tag{10}$$

where v represents the inlet velocity of coolant; n represents the number of cooling ribs; H represents the height of the cooling ribs; ω_1, ω_2, ω_3 represent the corresponding weighting factors, and $0\le\omega_1, \omega_2, \omega_3\le1$, $\omega_1+\omega_2+\omega_3=1$. $T_{\max}$ represents the maximum value of the temperature; $\Delta T_{\max}$ represents the maximum value of temperature difference between the U-W phase; $\Delta P_{\max}$ represents the maximum value of the pressure difference.

The optimization function can be expressed as

$$F_{opt}(v^{obj},n^{obj},H^{obj})=\min(\omega_1\frac{T}{T_{\max}}+\omega_2\frac{\Delta T}{\Delta T_{\max}}+\omega_3\frac{\Delta P}{\Delta P_{\max}}) \tag{11}$$

where v^{obj}, n^{obj}, H^{obj} are the inlet velocity of cooling liquid, the number of cooling ribs and the height of cooling ribs corresponding to the optimal objective function respectively.

2) Fruit Fly Optimization Algorithm

The fruit fly optimization algorithm (FOA) is a swarm intelligence global optimization method. Its search process simulates the fruit fly foraging process, and the optimal solution is obtained by iterative search of food sources. FOA has simple principle, less adjustment parameters, fast convergence speed and high operation efficiency. Hence, FOA is used to obtain the minimum value of the objective function in this paper. The process of FOA is as follows

Step 1: Initialize swarm's location.

$$\begin{cases} Init & X\_axis \\ Init & Y\_axis \end{cases} \tag{12}$$

where X_axis and Y_axis determines the swarm's initial position.

Step 2: Calculate each fruit fly's position.

$$\begin{cases} X_i = X\_axis + random(D) \\ Y_i = Y\_axis + random(D) \end{cases} \tag{13}$$

Each fly group has a specific range, denoted D, to determine how far a fruit fly can move in each iteration, measured by the maximum distance between the position of each fruit fly and swarm's initial location. The ith fruit fly's position is collectively determined by X_i and Y_i.

Step 3: Calculate the food smell.

$$\begin{cases} Dist_i = \sqrt{X_i^2 + Y_i^2} \\ S_i = \dfrac{1}{Dist_i} \\ Smell_i = Fitness(S_i) \end{cases} \tag{14}$$

Typically, $Dist_i$ measures the distance between the origin and the ith fruit fly. S_i stands for food concentration. S_i is determined by $Dist_i$ and stands for food concentration. $Smell_i$ is the smell concentration perceived by current fruit fly. *Fitness()* is used to numerically evaluate each individual fruit fly. Based on this *Fitness()* value, the best fruit fly can be selected across all the iterations.

Step 4: Identify the optimal solution.

$$[Smell_{best}\ Position_{best}] = \min(Smell_i) \tag{15}$$

Step 5: Update the swarm's location.

$$\begin{cases} X\_axis = X\_position \\ Y\_axis = Y\_position \end{cases} \tag{16}$$

where $X\_position$ and $Y\_position$ determines the swarm's position after update.

Step 6: Update the swarm's location.

Iterative steps 2-5 until the optimal target is reached.

3) Optimal Results and Analysis

FOA is used to iteratively search the minimum value of objective function, and obtain the optimal velocity of coolant, the number of cooling ribs and the height of ribs. The number of iterations is set to 100. The population size is set to 50. Table Π shows the optimization results under different weights. If the minimum temperature of the cooling plate and the minimum temperature difference between the U-W phases are taken as the objectives, the optimal inlet velocity is 7 m/s, but the pressure loss at this time reaches the maximum. If the objective is to minimize the pressure loss, the optimal coolant velocity is 1 m/s, but the objective function is as high as 0.446. By weighing the relationship among the optimal velocity, the optimal number of radiator ribs and the optimal height of radiator ribs, it is assumed that the three factors have the same influence on the temperature of the controller. Taking their weights as 1/3, the objective function value is 0.394. At this time, the function value is the smallest and the heat dissipation effect is the best. The corresponding optimal number and height of cooling ribs and inlet velocity of coolant are 5, 7.5 mm and 4 m/s respectively.

TABLE II
RESULT OF MULTI-OBJECTIVE OPTIMIZATION

Weighting factor	Objective function	Optimal velocity	Optimal number	Optimal height
$\omega_1=1, \omega_2=\omega_3=0$	0.715	7	7	7.5
$\omega_2=1, \omega_1=\omega_3=0$	0.446	1	1	7.5
$\omega_3=1, \omega_1=\omega_2=0$	0.584	7	0	7.5
$\omega_1=\omega_2=\omega_3=1/3$	0.394	4	5	7.5

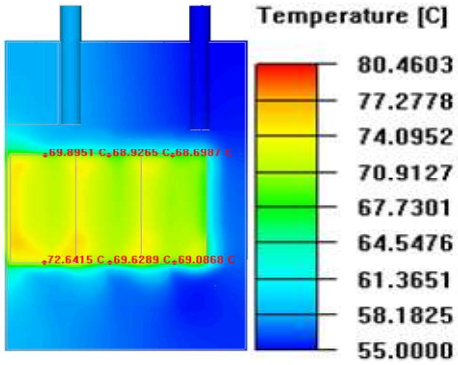

Fig. 8. Substrate temperature cloud map.

Finally, a set of data with the best heat dissipation performance is selected as the structural parameters of the cooling radiator. According to the setting of Part IV, the water cooled radiator is analyzed. The temperature distribution of the radiator bottom plate and IGBT is shown in Fig. 8. It can be seen from the diagram that the lowest temperature appears on the inlet side because the cooling method of the heat dissipation plate is water cooled. It can be seen from the temperature distribution of the water cooled cooling plate that the temperature difference between the hot end of the cooling plate (the part close to IGBT) and the cold end of the cooling plate (excluding the other parts of the hot end) is small, and the temperature distribution is uniform, showing excellent thermal conductivity. In the simulation, two temperature monitoring points are set in each of the three IGBTs. and the temperature at the two ends of the three IGBTs are 68.70 °C, 69.09 °C, 68.93 °C, 69.63 °C, 69.90 °C, 72.64 °C respectively. The temperature rise is 13.70 °C, 14.09 °C, 13.93 °C, 14.63 °C, 14.90 °C, 17.64 °C respectively. The maximum temperature of the water cooled radiator is 80.46 °C, which appears at the end of the third IGBT far from the outlet.

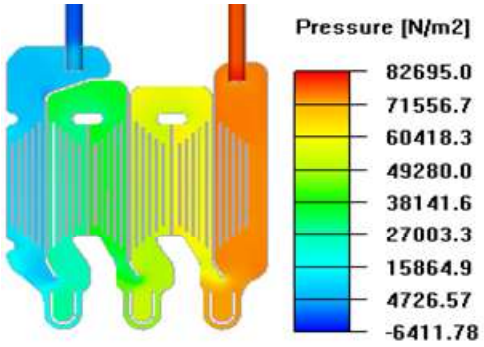

Fig. 9. Cloud map of pressure distribution.

Fig. 9 shows the pressure distribution of the water cooled radiator. The pressure at the water inlet is the largest and the pressure at the water outlet is the smallest. The maximum pressure is 82695 N/m^2. Because of the cooling reflux, the pressure at the water outlet is negative, about - 6411.8 N/m^2.

TABLE III
PERFORMANCE COMPARISON BEFORE AND AFTER OPTIMIZATION

	Before optimization	Optimized	Optimization proportion
T_{max}	88.3459 °C	80.4603 °C	8.9%
ΔT	33.3459 °C	25.4603 °C	23.6%
ΔP	128629 N/m^2	76283 N/m^2	40.7%

The performance comparison before and after optimization are shown in Table III. It can be seen that the maximum temperature of the radiator is reduced from 88.3459 °C to 80.4603 °C, which is reduced by nearly 9% .Also, the temperature difference between phase U and W is reduced by 23.6%. The safety and stability of the controller are improved significantly after optimization. The pressure difference between inlet and outlet is reduced from 128629N/m^2 to 76283N/m^2, which is reduced by 40.7%. It effectively reduces the power loss of the pump and improve the efficiency of the whole system.

B. Experimental Verification

In order to further verify the heat dissipation performance of the optimized cooling radiator, a prototype according to the optimization results was manufactured, and necessary experiments were carried out, as shown in Fig. 10.

The experimental setup mainly includes the water cooled radiator, the alternative heat source, the display instrument, water pump and temperature sensor. The temperature of each test point is recorded when the temperature becomes stable.

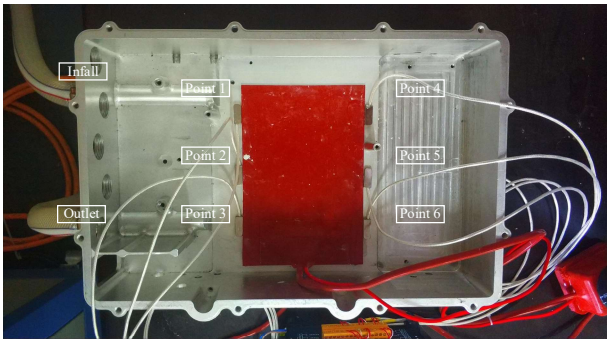

(a)

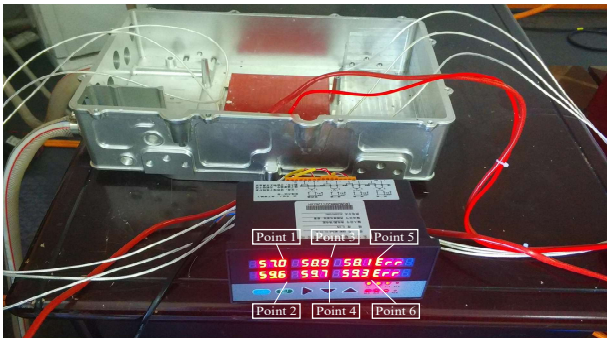

(b)

Fig. 10. The prototype and experimental setup.

Table IV shows the comparison between the experimental and simulation results. It can be seen from Table 4 that the temperature rise obtained by simulations and experiments have good similarity, which verifies the effectiveness of the proposed method. The maximum error between the simulation and the experimental results is 3.34 °C, and the experimental temperature rise is lower than that of simulations. It is because the temperature sensor is partially exposed to the air in the experiment, and the air takes away part of the heat. Besides that, there is a certain error caused by the finite element method.

TABLE IV
COMPARISON OF TEMPERATURE RISE OBTAINED BY EXPERIMENTS AND SIMULATIONS

Point	1	2	3	4	5	6
Experiment /°C	12.00	14.60	13.70	14.70	13.10	14.30
Simulation /°C	13.70	14.09	13.93	14.63	14.90	17.64

VI. CONCLUSIONS

In this paper, the heat dissipation performance of the water cooled radiator for a new energy vehicle motor controller is analyzed using finite element analysis in both the temperature field and fluid field. The sensitivity analysis of the structural parameters on the maximum temperature rise, the temperature difference and the coolant pressure loss is also investigated. The relationship between the number of cooling ribs, coolant flow rate and the height of cooling ribs to the maximum temperature, temperature difference and pressure loss of the cooling system is obtained, which provides a reference for the optimal design of heat dissipation system. The multi-objective optimization is transformed into a single objective optimization by linear weighting method, and the fruit fly optimization algorithm is proposed to obtain the optimal design parameters. The effectiveness of the proposed optimization method is verified by comparing the performance of heat dissipation system before and after optimization. The performance is improved significantly by optimizing the coolant velocity, the number and the height of the cooling ribs.

REFERENCES

[1] Cui Xiaofa, Wang Kai, "Analysis of three Key Technologies and Difficulties of New Energy Vehicles," *Auto Parts*, vol. 11, no. 03, pp. 81-83, Mar, 2018.

[2] Hu Xiaoxiao, "Opportunity and Development Trend of new energy vehicle technology Development," *Automotive practical technology*, vol. 44, no. 18, pp. 22-24, Sep, 2019.

[3] Dong Weijie, MENG Xiaoli, SONG Xiaohui, LI Wei, "Design and Simulation of IGBT Radiators," *Journal of system simulation*, vol. 28, no. 09, pp. 32-36, Sep, 2013.

[4] Liu Huanlong, ZHENG Zhong, Chen Jianming, "Heat Dissipation characteristics of vehicle Motor Controllers based on heat fluid-solid coupling," *Machine Tool & Hydraulics*, vol. 47, no. 13, pp. 152-156+178, Abbrev. Jul,2019.

[5] Guo Jianhong, Li Zhenguo, Fu Deping, "Research on evaporative cooling technology of high-power Power electronic devices," *Power Electronics Technology*, vol. 39, no. 05, pp. 141-143, Oct, 2005.

[6] Chen Guodong, Liu Hong, Wang Jiangtao, "Optimization design of heat dissipation of PEBB unit based on curve fitting," *Journal of electrical technology*, vol.31, no. 04, pp. 71-78, Feb,2016.

[7] Ren Huili, WANG Xuelin, Hu Yujin, Li Chenggang, "Dynamic Response Simulation analysis of crane system in a crane," *Journal of System Simulation*, vol. 19, no. 12, pp. 2665-2668, Jun, 2007.

[8] Yin Liaofei, Jiang Peixue, Xu Ruina, Hu Haowei, "Water flow boiling in a partially modified microgap with shortened micro pin fins," International Journal of Heat and Mass Transfer, vol. 155, no. C, Jul, 2020.

[9] Bai Baodong, Chen Dezhi, WANG Xinbo, "Calculation of inverter IGBT loss and design of cooling device," *transactions of chinese electrotechnical society*, vol. 28, no. 08, pp. 97-106, Aug, 2013.

[10] Hu Jianhui, Li Jingeng, Zou Jibin, Tan Jiubin, "Calculation of loss of IGBT module in inverter and design of heat dissipation system," *Transactions of China Electrotechnical Society*, vol. 24, no. 03, pp. 159-163, May, 2009.

[11] Wang Zhuo, XIA Guodong, MA Dandan, Yang Yuchen, "Study on fluid flow and heat transfer characteristics in single-layer and double-layer microchannels," *Journal of Engineering Thermophysics*, vol. 40, no. 05, pp. 1126-1130, May, 2019.

[12] Wang Shuwang, LU Ling, LAI Jianbin., "Calculation method and Verification of IGBT Junction Temperature of Electric vehicle Motor Controller," *Journal of Hefei University of Technology*, vol. 42, no. 03, pp. 370-375, Mar, 2019.

[13] Jie Guisheng, SUN Chi, WANG Guangsen, Nie Ziling, MENG Qingyun, "Optimization Design of Plate Water Cooling Radiator in Large Capacity Power Electronic Device," *Journal of Mechanical Engineering*, vol. 46, no. 02, pp. 99-105,Jan, 2010.

[14] Lv Jiangwei, ZHOU Kai, "Optimum Width Ratio of High Power Density Linear Switched Reluctance Motor," *Journal of Tsinghua University*, vol. 58, no. 05, pp. 469-476, Feb, 2016.

[15] DENG Huanyu,CHANG Shinan,SONG Mengjie, "The optimization of simulated icing environment by adjusting the arrangement of nozzles in an atomization equipment for the anti-icing and deicing of aircrafts," *International Journal of Heat and Mass Transfer*, vol. 155, no. C, Jul,2020.

Zhang Zhu received his B.Sc. From Hunan Institute of Engineering in 2004, M. S. degree in power electronics from South China University of Technology in 2007, Ph.D. in electrical engineering from The Hong Kong Polytechnic University in 2012. Now he is a lecturer with Hunan University of Science and Technology. He is the author of more than 30 articles. His research interests include power electronics and power transmission, intelligent control etc.

Liu Yunfan received his B.Sc. degree from Hunan Institute of Engineering in 2019.Now he is a M.Sc. candidate at Hunan University of Science and Technology. His main research interests include power electronics and electrical driver system.

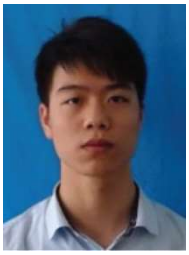

Wang Jingyuan received his B.Sc.degree from Hubei University of Science and Technology in 2018.Now he is a M.Sc. candidate at Hunan University of Science and Technology. His main research interests include power electronics and electrical driver system.